Excess entropy scaling of transport properties in network-forming ionic melts (SiO2 and BeF2)

ARTICLE *in* THE JOURNAL OF CHEMICAL PHYSICS · JANUARY 2011

Impact Factor: 2.95 · DOI: 10.1063/1.3521488

4 AUTHORS, INCLUDING:

Murari Singh
Weizmann Institute of Science
8 PUBLICATIONS **82** CITATIONS
SEE PROFILE

Charusita Chakravarty
Indian Institute of Technology Delhi
106 PUBLICATIONS **1,876** CITATIONS
SEE PROFILE

Excess entropy scaling of transport properties in network-forming ionic melts (SiO_2 and BeF_2)

Manish Agarwal,[1] Murari Singh,[2] B. Shadrack Jabes,[1] and Charusita Chakravarty[1,a)]
[1]*Department of Chemistry, Indian Institute of Technology-Delhi, New Delhi 110016, India*
[2]*School of Physical Sciences, Jawaharlal Nehru University, New Delhi 110067, India*

(Received 27 July 2010; accepted 8 November 2010; published online 3 January 2011)

The regime of validity of Rosenfeld excess entropy scaling of diffusivity and viscosity is examined for two tetrahedral, network-forming ionic melts (BeF_2 and SiO_2) using molecular dynamics simulations. With decrease in temperature, onset of local caging behavior in the diffusional dynamics is shown to be accompanied by a significant increase in the effect of three-body and higher-order particle correlations on the excess entropy, diffusivity, ionic conductivity, and entropy-transport relationships. The signature of caging effects on the Rosenfeld entropy scaling of transport properties is a distinctly steeper dependence of the logarithm of the diffusivity on the excess entropy in ionic melts. This is shown to be true also for a binary Lennard-Jones glassformer, based on available results in the literature. Our results suggest that the onset of a landscape-influenced regime in the dynamics is correlated with this characteristic departure from Rosenfeld scaling. The breakdown of the Nernst–Einstein relation in the ionic melts can also be correlated with the emerging cooperative dynamics.
 [doi:10.1063/1.3521488]

I. INTRODUCTION

Relating structure, thermodynamic, and transport properties of fluids is important in a variety of contexts. Recent work suggests that an effective route for making such connections is through the excess entropy (S_e), defined as the difference between the total thermodynamic entropy (S) and the corresponding ideal gas entropy (S_{id}).[1–20] Structure and entropy can be related using multiparticle correlation expansions of the entropy.[21–23] Semiquantitative relationships between transport properties and the excess entropy were originally formulated for simple liquids by Rosenfeld.[24–27] Such scaling relationships are of the form $X^* = A\exp(\alpha S_e)$, where X^* are dimensionless transport properties with either macroscopic (Rosenfeld) or microscopic (Dzugutov) reduction parameters, and A and α are scaling parameters. The relationships are quasiuniversal, corresponding states type of relations where the scaling parameters, A and α, are identical for systems with conformal potentials. For example, in the case of simple liquids, using macroscopic Rosenfeld scaling parameters the scaled diffusivities (D^*) obey the relation

$$D^* = D\frac{\rho^{1/3}}{(k_BT/m)^{1/2}} = 0.6\,\exp(0.8S_e), \tag{1}$$

where D is the unscaled diffusivity, ρ is the number density, T is the temperature, m is the particle mass, and S_e is measured in units of k_B per particle.[26]

An exponential scaling relationship between a dimensionless transport property and excess entropy is referred to here as Rosenfeld scaling. Such a scaling form is expected to be valid in the dense fluid, where diffusion proceeds through a combination of binary collisions and cage relaxations. This scaling form can be intuitively justified by noting that the binary collision contribution can be approximately factored out by using macroscopic reduction parameters based on elementary kinetic theory, provided that an effective hard-sphere radius can be assigned to the constituent particles. The frequency of cage relaxations will then be proportional to the number of accessible configurations, $\exp(\alpha S_e)$, since configuration space connectivity is high in the stable liquid phase. The state-point independent character of the scaling relationship implies that the exponential parameter α controlling the number of accessible configurations is determined only by the interaction potential and will be otherwise state-point independent. Energy landscape analysis suggests that while this last assumption is very plausible for simple liquids, it is not necessarily so for complex fluids.[28,29]

Recent simulations show that entropy scaling relationships are applicable to a much wider variety of liquids than was originally assumed, including water,[15] ionic melts,[2,13,14] core-softened fluids,[2,6,7,10,30] model polymeric melts,[12] and room-temperature ionic liquids.[20] Experimental data on molecular fluids (H_2O, CO_2 and N_2) show that Rosenfeld scaling holds for both the stable and the dense supercritical fluid, suggesting that such a scaling relationship may prove useful in predicting properties of fluids under high temperature and pressure conditions.[31–33] Since Rosenfeld entropy scaling relationships have been shown to be an effective means of relating thermodynamic and dynamic properties of fluids, it is important to clearly define its regime of validity. It is well-known that the exponential scaling regime breaks down in the low-density limit where Enskog theory is valid.[26] Both simulations and experiments suggest that the scaling relationships hold for the dense fluid in the stable liquid as well as supercritical regime. It is also

a)Author to whom correspondence should be addressed. Electronic mail: charus@chemistry.iitd.ac.in. Tel: (+)91-11-2659-1510. Fax: (+)91-11-4716-5550

well-established that Adam–Gibbs scaling provides an effective description of the relationship between mobility and thermodynamics in strongly supercooled liquids.[34] Therefore the relationships between structural correlations, entropy, and transport properties must change qualitatively as the system transits from the stable to supercooled liquid regimes with corresponding deviations from Rosenfeld-scaling behavior.

In this work, we focus on understanding the temperature–density regime where Rosenfeld scaling may be expected to break down as configuration space connectivity is diminished due to cooling. We focus primarily on molecular dynamics simulations of two network-forming ionic melts, BeF_2 and SiO_2; in addition, we provide a brief comparison with the behavior of the binary Lennard-Jones glassformer.[35,36] We note that entropy scaling in this regime has been previously studied using isotropic potentials for water, and a room-temperature ionic liquid. In both cases, an analogous breakdown of Dzugutov scaling was associated with significant departures from Gaussian diffusive behavior.[20,37] The studies were limited to a single isobar or isochore and used a pair-correlation approximation to the excess entropy. Our study extends the previous work by using the thermodynamic excess entropy, S_e, which includes the effect of all types of structural correlations on the entropy and minimizes the state-point dependence of the entropy-scaling parameters.[15] By choosing an ionic melt as our system, we are able to also examine the behavior of the ionic conductivity.

Molten beryllium fluoride (BeF_2) and silica (SiO_2) may be considered as representative of the general class of tetrahedral liquids with waterlike anomalies, including water, and silicon. Rosenfeld scaling in such systems is of interest because it provides the crucial connection between thermodynamic and transport anomalies. A necessary condition for the existence of waterlike anomalies is the existence of an excess entropy anomaly, corresponding to a rise in S_e on isothermal compression.[2–11,16,17] Provided Rosenfeld scaling holds and the strength of the entropy anomaly is sufficiently strong, anomalous increases in various measures of mobility on isothermal compression will be seen. The structural origins of such excess entropy anomalies lie in a transition between two distinct symmetries or length scales for local order as a function of density. For example, in BeF_2 and SiO_2, the low-density liquid is dominated by local tetrahedral order determined by the cation–anion radius ratio and reflected in the corresponding crystalline forms, such as quartz and coesite.[16] At high densities, a transition to local order consistent with coordination numbers greater than 4 takes place, corresponding to the local octahedral coordination seen in the stishovite phase of SiO_2. Intermediate densities correspond to regimes where structural frustration and the excess entropy reach a maximum. Structure, entropy, and transport relationships in ionic melts are also of interest because of the importance of structure–viscosity–conductivity in practical applications. In the case of BeF_2 and SiO_2, previous studies have noted an unexpected breakdown of the Nernst–Einstein relation in the low-temperature, low-density regime connecting the single-particle diffusivities with ionic conductivity.[13,14] Simulation details for BeF_2 and SiO_2 are summarized in Sec. II of the paper. Results are discussed in Sec. III and conclusions in Sec. IV.

II. COMPUTATIONAL DETAILS

Molecular dynamics simulations of ionic melts (BeF_2 and SiO_2) were performed in the canonical (NVT) ensemble using the Verlet algorithm as implemented in the DL_POLY package[38] using the transferable rigid-ion model (TRIM) potential for BeF_2 (Ref. 39) and the van Beest–Kramer–van Santen (BKS) potential for SiO_2.[40,41] The potential parameters as used in this work are summarized in Ref. 3. In the case of BeF_2, the temperature range studied was 1500–3000 K and the density range was from 1.5 to 3.0 g cm^{-3}; the temperature and density ranges for SiO_2 were 4000–6000 K and 1.8–4.2 g cm^{-3}. Details of simulations of the two ionic melts are given in Ref. 14. When estimating the entropies of the ionic melts, S_{id} was computed for a noninteracting multicomponent mixture of atoms with the same masses and mole fractions as the ionic melt. The system size for BeF_2 and SiO_2 corresponded to 450 ions. This system size chosen is small enough that a large number of state points could be efficiently covered, but sufficiently large that finite-size effects would be expected to make only small quantitative differences to the computed values of thermodynamic and transport properties. The details of computation of transport properties, especially the ionic conductivity and viscosity, are given in Ref. 14.

Excess entropy for BeF_2 and SiO_2 melts were calculated using thermodynamic integration with the reference state defined as an binary ideal gas mixture with the same stoichiometry and atomic masses as the ionic melt. Since such an ideal gas reference system cannot be smoothly transformed into an ionic system with long-range Coulomb interactions, we used an intermediate binary Lennard-Jones following the procedure developed for SiO_2.[42–44] Details of the excess entropy estimations are given in Ref. 5, but the data presented here covers a more extensive density range.

III. RESULTS AND DISCUSSION

A. Rosenfeld scaling of transport properties

A Rosenfeld plot for excess entropy scaling of diffusivities corresponds to a linear dependence of the reduced diffusivity, D^*, on the excess entropy, S_e, in units of the Boltzmann constant, k_B. Figure 1 shows the Rosenfeld-scaling plot of two ionic melts, SiO_2 and BeF_2. The data from the high temperature isotherms for each system fall on a straight line with a slope of 1.31 for BeF_2 and 1.42 for SiO_2; a simple liquid would be expected to show a slope close to 0.8.[24] Note that there are small, systematic differences between scaling parameters for different isochores but the overall collapse of the data onto a high-temperature and a low-temperature line is clear. The data from the low-temperature isotherms, however, lies on a separate line with a slope of 5.53 and 4.42 for BeF_2 and SiO_2, respectively. This characteristic bend or knee, corresponding to a fairly sharp but not discontinuous transition to a regime with a larger value of α on supercooling, has been observed in simulations of simple liquids,[45] water,[15]

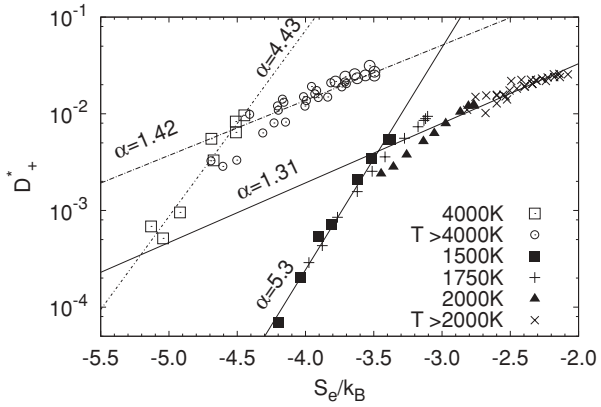

FIG. 1. Correlation of reduced cation diffusivities (D^*_+) in BeF_2 and SiO_2 melts with S_e. $D^*_+ = D_+\rho^{1/3}/(k_BT/m_+)^{1/2}$, where m_+ is the cation mass. The lines are exponential fits with the slopes as indicated. The open squares correspond to SiO_2 for the 4000 K isotherm and the open circles correspond to isotherms above 4000 K. The remaining symbols refer to simulations for the BeF_2 melt at different temperatures.

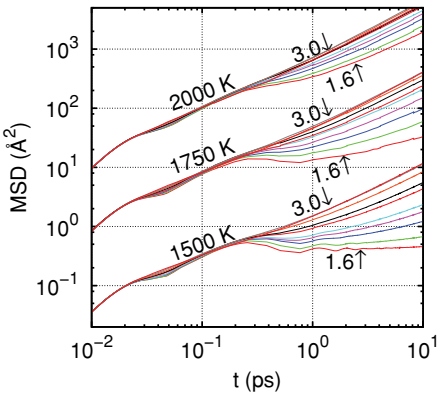

FIG. 2. Mean square displacements (MSDs) for several densities along the 1500, 1750, and 2000 K isotherms for BeF_2 melt. The 1750 and 2000 K MSDs are shifted up by multipliers of 20 and 200, respectively. The arrows indicate the lowest and highest densities along an isotherm in g cm^{-3}. The densities are 1.6–2.2 g cm^{-3} in increments of 0.1, and thereafter 2.4, 2.6, and 3.0 g cm^{-3}.

ionic melts (BeF_2 and SiO_2), and model glassformers (binary Lennard-Jones and binary hard-sphere systems).[7,8,13,15,45,46] In the case of simple liquids, binary glassformers, and the ionic melts, the data from various isochores collapse very well onto the same curve, while in the case of water there is a somewhat stronger isochore dependence of the scaling parameters.

B. Deviations from Gaussian diffusive behavior

The change in the slope of the Rosenfeld plot, indicating a sharp change in the exponential scaling parameter, has been suggested as indicating the onset of cooperative dynamics as signaled by departures from Gaussian diffusive behavior. This can be verified by examining the time dependence of the mean square displacement where a region of zero slope indicates the formation of a local cage with a finite lifetime and contains essentially the same information as the non-Gaussianity parameter studied elsewhere.[20,37]

In the case of BeF_2, the change in α is fairly sharp and occurs at $S_e \approx -3.5k_B$. For example, diffusivities from state points with density less than 2.3 g cm^{-3} along the 1750 isotherm correspond to S_e values below this threshold, while at 2000 K, S_e values for all state points lie above this threshold. Figure 2 shows the mean square displacement (Δr^2) as a function of time for several densities along the 1500, 1750, and 2000 K isotherms. Using a logarithmic scale on both axes, evidence of local caging effects can be seen as a plateau on the $\Delta r^2(t)$ plots. The onset of such a plateau is just visible for the MSD curves at the lowest densities along the 2000 K isotherm. The plateau regime becomes progressively more important at lower temperatures for a wider range of densities. Thus, the change in α is clearly correlated with the onset of significant caging effects on the single-particle diffusivities. Similar results are obtained for SiO_2 melt with the change in the slope of Rosenfeld scaling coinciding with onset of the caging effect occurring at approximately 4500 K. This is consistent with earlier suggestions based on mode-coupling analysis of dynamics in one- and two-component Lennard-Jones and hard-sphere systems as well as simulation studies on Dzugutov scaling in water and ionic melts.[2,37,45,47]

It is interesting to note that local caging effects in ionic melts take place at temperatures well above the melting temperature. For example, in the case of BKS silica, low-density state points along the 4500 K isotherm show caging effects on the diffusional dynamics although the melting temperature of the low-pressure cristobalite phase is 2000 K and that of the high-pressure coesite phase is 3000 K. This was originally noted by Horbach and Kob.[48] While the phase diagram of the TRIM model of BeF_2 has not been computed, the experimental melting temperature is 813 K. Clearly, in such network-forming melts, few-body cooperative effects become important even in the liquid phase, while in simple liquids and glassformers they become observable only in the supercooled regime.

C. Excess and pair-correlation entropy

For a mixture of unstructured particles with isotropic interactions, the pair entropy contribution to the excess entropy can be written as[23]

$$S_2/Nk_B = -2\pi\rho \sum_{\alpha,\beta} x_\alpha x_\beta \int_0^\infty \{g_{\alpha\beta}(r)\ln g_{\alpha\beta}(r) - [g_{\alpha\beta}(r) - 1]\} r^2 dr, \quad (2)$$

where $g_{\alpha\beta}(r)$ is the pair-correlation function between spherically symmetric particles of type α and type β and x_α is the mole fraction of particles of type α. Considering an AB_2 ionic melt as a binary mixture of A and B ions interacting via isotropic pair interactions, we can apply the above formula to obtain the pair correlation entropy, S_2. Contributions due to higher-order multiparticle correlations are represented as the residual multiparticle entropy (RMPE) defined as $\Delta S = S_e - S_2$. The correlation plots between S_2 and S_e for BeF_2 and SiO_2, shown in Fig. 3, indicate that there is a quasilinear correlation between the two quantities, with

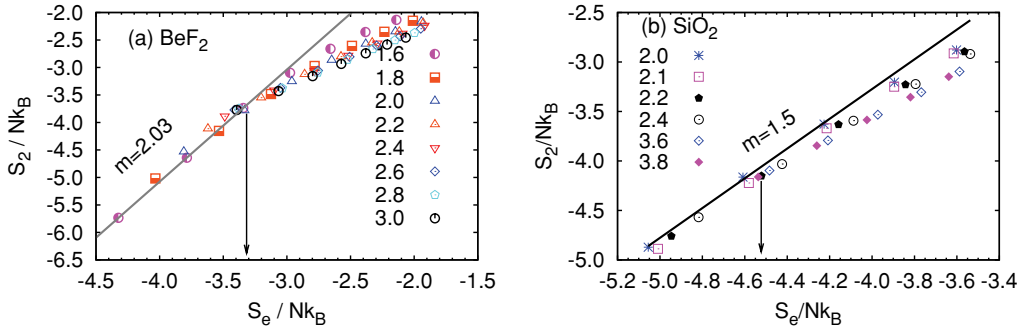

FIG. 3. Correlation plot between pair entropy S_2 and excess entropy S_e is shown for (a) BeF_2 and (b) SiO_2, along various isochores. The straight lines labeled by the slopes (m) represent a linear fitting of the data points lying along the lowest density isochore.

a distinct change in slope when $S_e \approx -3.5k_B$ for BeF_2 and $S_e \approx -4.5k_B$ for SiO_2, which coincides with the onset of local caging effects as well as the break in the Rosenfeld-scaling plots discussed above. While there is no abrupt transition at S_e values associated with the change in the exponential scaling parameter, there is a qualitative change in the structural correlations indexed by the RMPE contribution that must affect the dynamics.

The RMPE represents the effect of three-body and higher-order correlations in ionic melts and typically contributes 10%–20% of S_e. The temperature and density dependence of the RMPE for the two ionic melts studied here was examined in a previous study and shown to be very similar.[5] Based on the earlier study, we can show that for S_e values lower than $-3.5k_B$ and $-4.5k_B$ for BeF_2 and SiO_2, respectively, the RMPE is relatively strongly correlated with tetrahedral order. The effect of the RMPE on the excess entropy and the transport properties (see the next section) is stronger in BeF_2 than in SiO_2 which may be understood on the basis of stronger propensity for tetrahedral order due to smaller cation–anion radius ratio in the former.[16] It should also be noted that RMPE has a positive value in BeF_2 and a negative value in SiO_2, possibly reflecting the different role of the pair entropy in the two systems, or the somewhat different potential parametrizations.

D. Structural correlations and diffusivity

In order to demonstrate this, Fig. 4 shows the Rosenfeld-scaled diffusivities as a function of S_2 as well as ΔS. The correlation between $\ln D^*$ and S_2 shows deviations from linearity in the low-temperature/low-density regime but there is no abrupt change in slope similar to that seen in Fig. 1. The differences between scaling with S_e and S_2 can be understood by considering Fig. 4(b). RMPE values greater than $0.4k_B$ correspond, in the case of BeF_2, to state points well within the anomalous liquid regime and are strongly correlated with the scaled diffusivity. For smaller magnitudes of the RMPE, the diffusivity is uncorrelated with the RMPE, indicating that the structural correlations associated with the onset of local caging effects, as reflected in the MSDs, have a crucial effect on the single-particle diffusivity. The results for diffusivity scaling with S_2 and ΔS for SiO_2 are shown in Fig. 5 and are essentially parallel to those for BeF_2, although the numerical range of diffusivities is lower.

In this context, it is important to consider the diffusivity scaling with respect to S_2, rather than S_e. Our previous work on BeF_2 and SiO_2 shows that $\log(D^*)$ vs S_2 does not show as sharp a break as $\log(D^*)$ vs S_e.[13] By using S_e, and monitoring the effect of RMPE on the diffusivity, we are able to demonstrate that the three-body and higher-order correlations become much more significant with onset of cooperative dynamics. In the case of BeF_2, and presumably other tetrahedral liquids, three-body correlations will be strongly connected with tetrahedral order, which is strongest in the low-density, low-temperature part of the phase diagram.[5] In the case of water, replacing the excess entropy by the pair entropy leads to a strong isochore dependence of the scaling parameters; the corresponding changes in the diffusional behavior will be published elsewhere.[15] In the study of isotropic water models, state-point-dependent potentials were constructed for

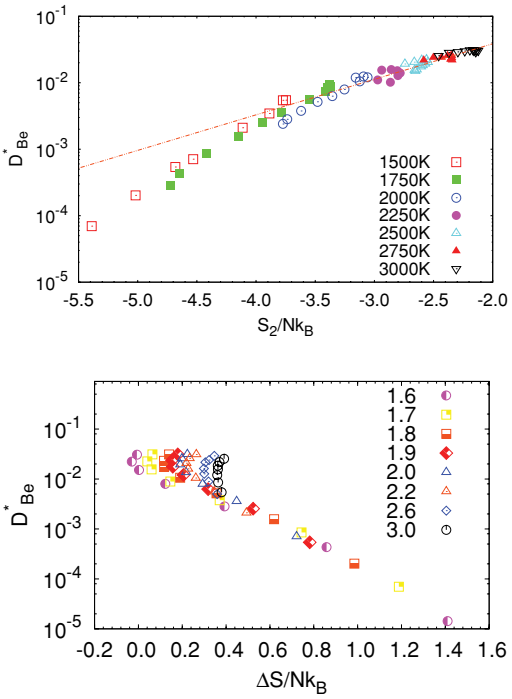

FIG. 4. Correlation of reduced diffusivities (D_+^*) in BeF_2 with (a) pair entropy, S_2 and (b) residual multiparticle entropy, ΔS

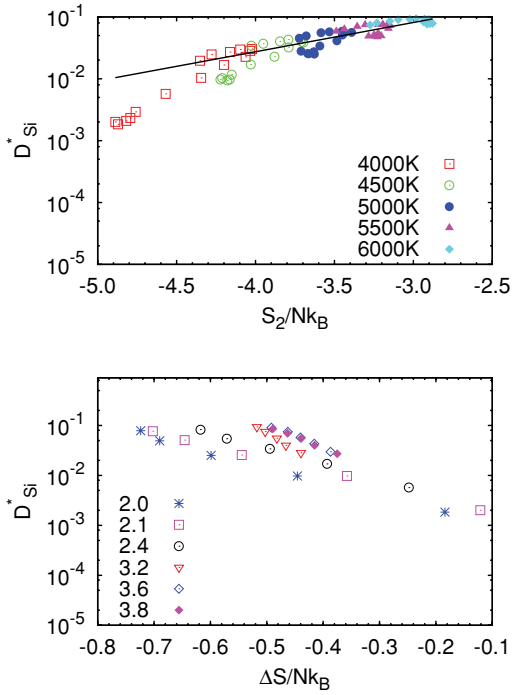

FIG. 5. Correlation of reduced diffusivities (D^*_+) in SiO_2 with (a) pair entropy, S_2 and (b) residual multi-particle entropy, ΔS.

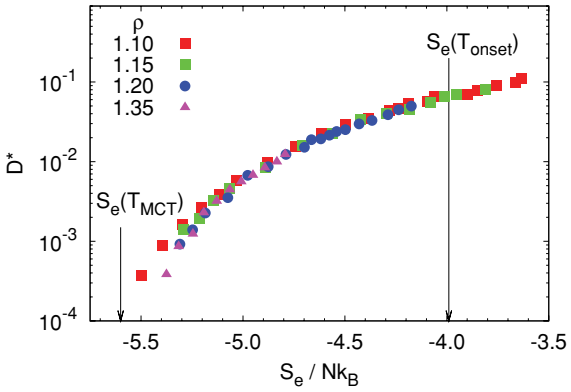

FIG. 7. Correlation of D^* and excess entropy S_e. The mode coupling temperature, T_{MCT}, and the onset temperature, T_{onset}, are marked by arrows.

water and therefore the change in the scaling parameters is more difficult to interpret in simple structural terms.[37] In the case of RTILs, a stronger dependence on S_2 is seen than in BeF_2, possibly because of the rigid body, asymmetric structure of the constituent ions which requires that the excess entropy is approximated by orientation-dependent PDF-based measures of entropy.

E. Structural correlations and the Nernst–Einstein relation

The relationship between structure–conductivity–viscosity plays a crucial role in applications of ionic melts. The viscosity and diffusivity are connected through the Stokes–Einstein relationship, which is found to hold for the silica and beryllium fluoride melts in the temperature and density range studied here.[4,14] The conductivity and the diffusivity are connected via the Nernst–Einstein relationship

$$\sigma = (e^2\rho/k_BT)(x_+z_+^2D_+ + x_-z_-^2D_-)(1-\Delta), \qquad (3)$$

where e is the electronic charge, $x_\pm$ and $z_\pm$ are the ionic mole fractions and charges, respectively, and Δ is the Nernst–Einstein deviation factor. Previous work shows that there is a striking breakdown of this relation for SiO_2 and BeF_2 at low temperatures and densities when the tetrahedral network is fairly robust.[13,14] The decoupling of the diffusivity and the ionic conductivity is indexed by the Nernst–Einstein deviation factor, Δ_{NE}, which is shown as a function of ΔS in Fig. 6. For state points, with S_e below the threshold value at which the Rosenfeld plot shows a change in slope [$S_e(BeF_2) < -3.5k_B$, $\Delta S(SiO_2) > 0.4k_B$], Δ_{NE} shows a strong, negative correlation with ΔS.

F. Comparison with the binary Lennard-Jones glassformer

The Kob–Andersen model of a binary Lennard-Jones glassformer has been extensively studied, particularly along certain specific isochores. We have used the diffusivity and the excess entropy from Ref. 35 to construct the Rosenfeld plot, shown in Fig. 7. The data from isochores with densities lying between 1.08 and 1.35 collapse very well on the same curve, though the figure shows only the ρ =1.1, 1.15, 1.2, and 1.35 isochores. This suggests that the excess entropy is indeed a crucial factor in controlling the transport properties, although the exponential scaling parameter increases continuously on supercooling. The change in α on supercooling is less sharp than in the tetrahedral ionic melts, possibly because

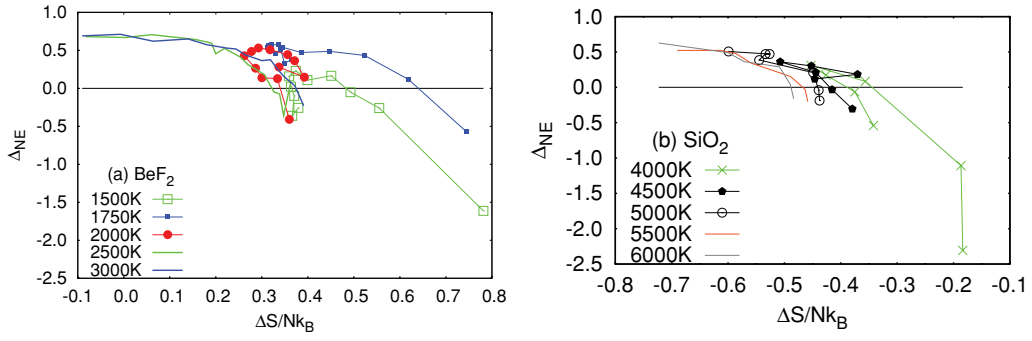

FIG. 6. Correlation of Nernst–Einstein deviation factor Δ_{NE} and residual multiparticle entropy, ΔS for (a) BeF_2 and (b) SiO_2.

of structural differences in the underlying local order. The onset temperature, T_{onset}, for this system, corresponding to the landscape influenced regime, is $T^* = 1.0$ along the $\rho = 1.2$ isochore corresponding to the $S_e = -4.0$ value shown in the plot.[36] The collapse of the data from different isochores would suggest that the onset temperature for the other isochores occurs at similar S_e values; we plan to explore this aspect in future work.

IV. CONCLUSIONS

The presence of local cooperative dynamics in diffusional behavior can be judged by the presence of a region of zero slope in the logarithmic plot of the mean square displacement as a function of time, indicating that the particle is temporarily trapped or caged by its neighbours. The formation of such a plateau region signals the onset of non-Gaussian diffusional behavior due to local caging effects. In the case of BeF_2 and SiO_2, we show that a sharp change in the Rosenfeld exponential scaling parameter is associated with the onset of such cooperative dynamics but takes place at temperatures well above the melting temperature. The binary Lennard-Jones glassformers show a more continuous change in the exponential scaling parameter with supercooling than the ionic melts but the onset temperature is again correlated with deviations from Gaussian behavior of the diffusivity. For both systems, data from different isochores collapse on the same curve on the Rosenfeld plot. The formation of such a bend or "knee" in the Rosenfeld plot against excess entropy, seen in many liquids, is therefore likely to be a generic feature associated with onset of cooperative dynamics. In the case of network-forming ionic melt, the temperature of onset of such caging effects will be proportional to the energetic bias for locally ordered atomic environments. In the case of simple liquids, such local cooperative effects will be absent in the stable liquid phase and will be associated with supercooling leading to either nucleation or glass formation. Inherent structure analysis of such simple liquids describes weakly supercooled states as belonging to the "landscape-influenced" regime, rather than the "landscape-dominated" regime characteristic of strongly supercooled liquids.

The effect of multiparticle correlations on the entropy, diffusivity, viscosity, and ionic conductivity are examined in the temperature–density regime where deviations from Rosenfeld scaling are seen. We show that there is a rise in the importance of three-body and higher-order positional correlations in liquid BeF_2 associated with the onset of cooperative dynamics that affects both the entropy and the transport properties. The contribution of the residual multiparticle entropy to the excess entropy increases very significantly at the S_e value where the Rosenfeld plot shows a sharp change in the exponential scaling parameters. For state points with S_e greater than $-3.5k_B$, the RMPE contributes less than 10% while below this threshold the RMPE contribution rises steeply with temperature. The diffusivities, the viscosities, and the Nernst–Einstein deviation parameter are strongly correlated with the RMPE for state points with $S_e < -3.5k_B$. The correlation between the onset of cooperative effects and the dramatic breakdown of the Nernst–Einstein relation is quite striking. The behavior of SiO_2 melt is very similar to that of BeF_2 but the effects of three-body correlations and tetrahedral order are less striking.

The results on BeF_2, SiO_2, and binary Lennard-Jones presented here, in conjunction with results on simple one-component liquids, binary mixtures, tetrahedral liquids, and room-temperature ionic melts, suggest that deviations from Rosenfeld scaling will be associated with deviations from Gaussian diffusional behavior as the liquid enters the landscape influenced regime. The present study also relates these changes in dynamical behavior to the increased importance of multiparticle correlations in determining the excess entropy. The results for structural correlations would be expected to hold for other tetrahedral liquids, since the local tetrahedral order in these systems is favored with decreasing temperature and density and is associated with enhanced three-body correlations. The correlation in the breakdown of the Nernst–Einstein relation with the rise in RMPE will have interesting consequences for ionic melts, such as BeF_2, SiO_2, and LiF-BeF_2 mixtures. The nature of structural correlations in molecular fluids, with rigid or nearly, rigid molecules or molecular ions, as exemplified by water and room-temperature ionic liquids, may prove to be more complex and deserves further study.

ACKNOWLEDGMENTS

This work was financially supported by the Department of Science and Technology, New Delhi. M.A. and B.S.J. have been financially supported supported by the Indian Institute of Technology Delhi through Senior and Junior Research Fellowships, respectively. M.S. has been supported by a Junior Research Fellowship from the University Grants Commission. C.C. would like to thank P.G. Debenedetti, S.Sastry, and B. Bagchi for useful discussions. Some of this work was presented at the Kavli Institute of Theoretical Physics with partial support from the National Science Foundation under Grant No. NSF PHY05-51164.

[1] S. N. Chakraborty and C. Chakravarty, J. Chem. Phys. **124**, 014507 (2006).
[2] R. Sharma, S. N. Chakraborty, and C. Chakravarty, J. Chem. Phys. **125**, 204501 (2006).
[3] M. Agarwal, R. Sharma, and C. Chakravarty, J. Chem. Phys. **127**, 164502 (2007).
[4] M. Agarwal and C. Chakravarty, J. Phys. Chem. B **111**, 13294 (2007).
[5] R. Sharma, M. Agarwal, and C. Chakravarty, Mol. Phys. **106**, 1925 (2008).
[6] A. B. de Oliveira, G. Franzese, P. A. Netz, and M. C. Barbosa, J. Chem. Phys. **128**, 064901 (2008).
[7] J. Mittal, J. R. Errington, and T. M. Truskett, J. Chem. Phys. **125**, 76102 (2006).
[8] J. Mittal, J. R. Errington, and T. M. Truskett, J. Chem. Phys. **132**, 16994 (2010).
[9] J. Mittal, J. R. Errington, and T. M. Truskett, J. Phys. Chem. B **110**, 18147 (2006).
[10] J. R. Errington, T. M. Truskett, and J. Mittal, J. Chem. Phys. **125**, 244502 (2006).
[11] Z. Yan, S. V. Buldyrev, and H. E. Stanley, Phys. Rev. E **78**, 051201 (2008).

[12]T. Goel, C. N. Patra, T. Mukherjee, and C. Chakravarty, J. Chem. Phys. **129**, 164904 (2008).
[13]M. Agarwal and C. Chakravarty, Phys. Rev. E **79**, 030202 (2009).
[14]M. Agarwal, A. Ganguly, and C. Chakravarty, J. Phys. Chem. B **113**, 15284 (2009).
[15]M. Agarwal, M. Singh, R. Sharma, M. P. Alam, and C. Chakravarty, J. Phys. Chem. B **114**, 6995 (2010).
[16]B. S. Jabes, M. Agarwal, and C. Chakravarty, J. Chem. Phys. **132**, 234507 (2010).
[17]A. B. de Oliveira, E. Salcedo, C. Chakravarty, and M. C. Barbosa, J. Chem. Phys. **132**, 234509 (2010).
[18]R. Chopra, T. M. Truskett, and J. R. Errington, J. Phys. Chem. B **114**, 10558 (2010).
[19]Z. N. Gerek and J. R. Elliott, Ind. Eng. Chem. Res. **49**, 3411 (2010); see http://pubs.acs.org/doi/abs/10.1021/ie901247k.
[20]M. Malvaldi and C. Chiappe, J. Chem. Phys. **132**, 244502 (2010).
[21]H. S. Green, *The Molecular Theory of Fluids* (North-Holland, Amsterdam, 1952).
[22]A. Baranyai and D. J. Evans, Phys. Rev. A **40**, 3817 (1989).
[23]B. B. Laird and A. D. J. Haymet, Phys. Rev. A **45**, 5680 (1992).
[24]Y. Rosenfeld, Phys. Rev. A **15**, 2545 (1977).
[25]Y. Rosenfeld, Chem. Phys. Lett. **48**, 467 (1977).
[26]Y. Rosenfeld, J. Phys. Condens. Matter **11**, 5415 (1999).
[27]M. Dzugutov, Nature (London) **381**, 137 (1996).
[28]P. G. Debendetti and F. H. Stillinger, Nature (London) **410**, 259 (2001).
[29]D. J. Wales, *Energy Landscapes: With Applications to Clusters, Biomolecules, and Glasses* (Cambridge University Press, Cambridge, 2003).
[30]W. P. Krekelberg, T. Kumar, J. Mittal, J. R. Errington, and T. M. Truskett, Phys. Rev. E **79**, 031203 (2009).
[31]E. H. Abramson, Phys. Rev. E **76**, 051203 (2007).
[32]E. H. Abramson and H. West-Foyle, Phys. Rev. E **77**, 041202 (2008).
[33]E. H. Abramson, Phys. Rev. E **80**, 021201 (2009).
[34]P. G. Debenedetti, *Metastable Liquids: Concepts and Principles* (Princeton University Press, Princeton, NJ, 1996).
[35]S. Sastry, Phys. Rev. Lett. **85**, 590 (2000).
[36]S. Sastry, P. G. Debenedetti, and F. H. Stillinger, Nature (London) **393**, 554 (1998).
[37]M. E. Johnson and T. Head-Gordon, J. Chem. Phys. **130**, 214510 (2009).
[38]W. Smith, C. W. Yong, and P. M. Rodger, Mol. Simul. **28**, 385 (2002); the DLPOLY website is http://www.cse.clrc.ac.uk/msi/software/DL_POLY.
[39]L. V. Woodcock, C. A. Angell, and P. Cheeseman, J. Chem. Phys. **65**, 1565 (1976).
[40]B. W. H. van Beest, G. J. Kramer, and R. A. van Santen, Phys. Rev. Lett. **64**, 1955 (1990).
[41]I. Saika-Voivod, F. Sciortino, T. Grande, and P. H. Poole, Phys. Rev. E **70**, 061507 (2004).
[42]I. Saika-Voivod, P. H. Poole, and F. Sciortino, Nature (London) **412**, 514 (2001).
[43]I. Saika-Voivod, F. Sciortino, and P. H. Poole, Phys. Rev. E **63**, 011202 (2000).
[44]I. Saika-Voivod, F. Sciortino, and P. H. Poole, Phys. Rev. E **69**, 041503 (2004).
[45]C. Kaur, U. Harbola, and S. P. Das, J. Chem. Phys. **123**, 034501 (2005).
[46]M. Dzugutov, J. Phys. Condens. Matter **11**, A253 (1999).
[47]U. Harbola, C. Kaur, and S. Das, Phys. Rev. Lett. **91**, 229601 (2003).
[48]J. Horbach and W. Kob, Phys. Rev. B **60**, 3169 (1999).